Preprint Title	Divergent Role of PIDA and PIFA in the AlX_3 (X=Cl, Br) Halogenation of 2 Naphthol: A Mechanistic Study
Authors	Kevin A. Juárez-Ornelas, Manuel Solís-Hernández, Pedro Navarro-Santos, J. Oscar C. Jiménez-Halla and César R. Solorio-Alvarado
Publication Date	20 März 2024
Article Type	Full Research Paper
Supporting Information File 1	SI Cl and Br Article.pdf; 2.3 MB
ORCID® iDs	Manuel Solís-Hernández - https://orcid.org/0000-0002-1678-0107; César R. Solorio-Alvarado - https://orcid.org/0000-0001-6082-988X

Divergent Role of PIDA and PIFA in the AlX_3 (X=Cl, Br) Halogenation of 2 Naphthol: A Mechanistic Study

Kevin A. Juárez-Ornelas,[1] Manuel Solís-Hernández,[2] Pedro Navarro-Santos,[2,*] J. Oscar C. Jiménez-Halla[1*] and César R. Solorio-Alvarado,[1,*]

[1] Departamento de Quimica, Division de Ciencias Naturales y Exactas, Universidad de Guanajuato, Campus Gto, Noria Alta S/N 36050, Guanajuato, Guanajuato, Mexico.

[2] CONAHCYT - Instituto de Investigaciones Químico Biológicas, Universidad Michoacana de San Nicolás de Hidalgo. Francisco J. Mujica S/N 58030, Morelia, Michoacán, México.

Abstract

The chlorination and bromination reaction mechanisms of 2-naphthol under the previously reported PIDA- or PIFA-AlX_3 (X= Cl, Br) systems by our research group, was elucidated via quantum chemical calculations within the density functional theory. The studied chlorination mechanism using PIFA and $AlCl_3$ demonstrated better experimental and theoretical yields than when PIDA was used. Additionally, the lowest-in-energy chlorinating species involve an equilibrium between the Cl-I(Ph)-OTFA-$AlCl_3$ and [Cl-I(Ph)+] [-OTFA-$AlCl_3$] species more than the $PhICl_2$ formation. On the other hand, the bromination mechanism was more efficient using PIDA and $AlBr_3$ to form the intermediate Br-I(Ph)-OAc-$AlBr_3$ as the brominating active species. Similarly, the $PhIBr_2$ is higher-in-energy than our proposal. The detailed reaction mechanisms described in this work are in excellent agreement with the experimental yields. These initial results confirm that such mechanisms are energetically more likely to occur, forming the equilibrium species than in the presence of the corresponding halogenating $PhIX_2$.

* corresponding author: pnavarrosa@conacyt.mx, jjimenez@ugto.mx, csolorio@ugto.mx

Keywords: DFT calculations, iodine(III) reagents, aromatic chlorination and bromination.

1. Introduction

Hypervalent iodine(III) reagents have gained attention recently as low-toxic strong-oxidants[1] due to their ability to mimic some reactivity issues[2] of the transition-metal chemistry.[3] These compounds have been used in the formation of different types of bonds such as C - C,[4] C - O,[5] C - N,[6] C - S,[7] C–CN,[8] C-F,[9] C-I,[10] C-NO_2[11] and in the context of this work, C- X[12] (X= -Cl, -Br). Consistent with its diversified chemistry in organic synthesis, the application of different protocols for the halogenation of arenes using iodine(III) reagents have been described mainly using the systems PIDA-TMSCl, PIDA-TMSBr[13], and PIFA-TMSBr.[14] Recently, we developed a new protocol for the oxidative chlorination and bromination of naphthols using the systems PIFA-$AlCl_3$[12a] and PIDA-$AlBr_3$.[12c-d] These protocols combine iodine(III) reagents and aluminum salts to get the chlorination and bromination of electron-rich arenes under mild and operational easy conditions have not precedents (Scheme 1).

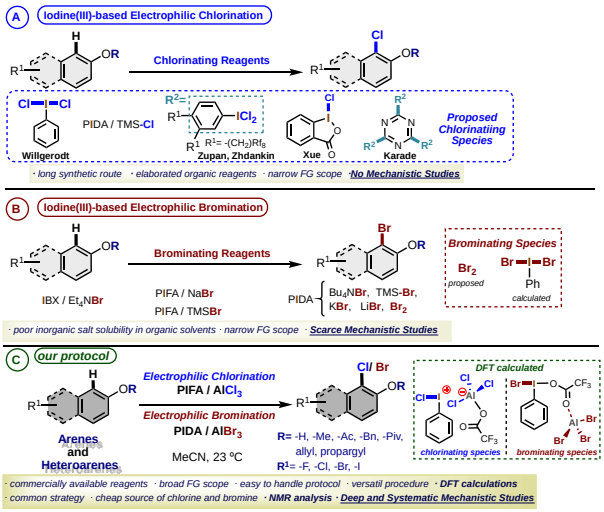

Scheme 1. Representative protocols for the oxidative aromatic chlorination and bromination using iodine(III)-based reagents.

The synthesis of aryl halides is of great importance in the knowledge of chemistry and for industrial interest. Recently, a new procedure developed in our research group showed the *ortho*-selective chlorination of phenols under mild conditions at short reaction times.[12a] The chlorinating species was generated *in situ* by simply mixing bis[(trifluoro-acetoxy)iodobenzene] (PIFA) with a Lewis acid, in this case, $AlCl_3$. The importance of this protocol arises from the oxidation of the chlorine atom coming from the $AlCl_3$, which is an

available and cheap reagent. Then, it is used as an electrophilic source in the chlorination process under an umpolung reactivity. In contrast to the suggested traceroute, where the chlorine or bromine atoms are attached to the hypervalent iodine center of the plausible reagent $PhIX_2$ (X= Cl, Br); our new protocols open broad paths for the reaction through different halogenating species. For a deeper understanding of these reactions, we explored different pathways of the reaction mechanisms for the *ortho*-halogenation using the 2-naphthol as a model (Eq. 1). In such a way, we found a reaction pathway that is energetically more favorable.

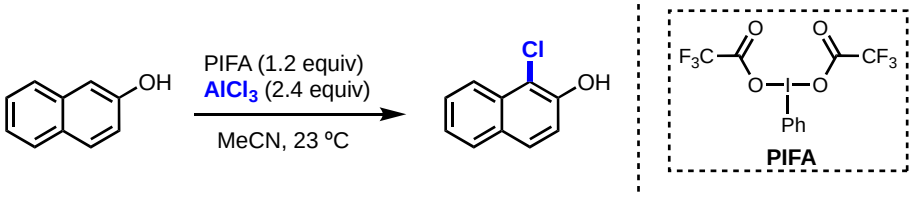

(1)

Based on our successful procedure for chlorination, we have also developed an efficient protocol for the electrophilic bromination of arenes, mainly phenols.[12c-d] Accordingly, the bromination reaction was initially explored by mixing PIFA-$AlBr_3$, which gave acceptable yields (84%). However, other iodine(III) reagents were tested as oxidants during the optimization process. Then, when using the mixture of (diacetoxyiodo)benzene (PIDA) with aluminum bromide (PIDA-$AlBr_3$), this resulted in a successful reaction, obtaining unexpectedly better yields (93%) than PIFA. Thus, the bromination reaction proceeded in the presence of PIDA-$AlBr_3$ as a brominating system using MeCN as solvent (Eq. 2).

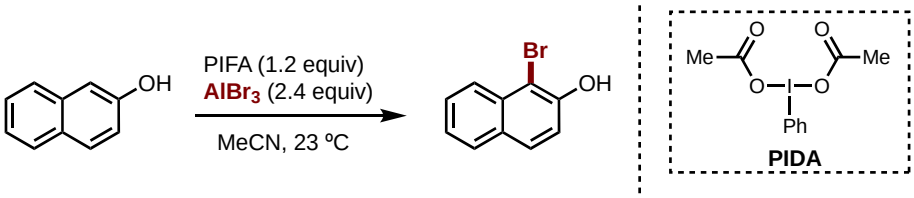

(2)

In light of the relevance regarding this newly discovered reactivity for the hypervalent iodine(III) reagents-aluminum salts and the scarce mechanistic and theoretical studies,[14] we computationally explored all of the different plausible pathways, elucidating the more feasible route that allowed the reported halogenation under these new reaction conditions. In this work, we systematically investigate the influence of PIDA and PIFA in the chlorination and bromination reactions, respectively. Interestingly, we found excellent agreement between the theoretical predictions and the experimental results.

2. Computational details

The equilibrium geometries of reagents and products, the stationary points and transition states structures were optimized by doing calculations in the framework of the Density Functional Density (DFT) employing the software Gaussian 16.[15] Although the B3LYP functional could be suitable for these calculations, i.e., to trace reaction pathways, dealing with nitrations of arenes, halogenations, nitrations, or FC acylations in solutions, we found the ω-B97XD functional[16] appropriate for this study because the ω-B97XD considers dispersion interaction through a range separation (22% for short range and 100% Hartree-Fock for long range), which properly describes the thermochemistry and non-covalent interactions. The electronic configurations of the molecules of these mechanisms were described with a Pople's split-valence basis set of double-ζ quality with one polarization function (for heavy atoms), 6-31G(d), for all the atoms. Geometry optimizations were carried out without any symmetry constraints, and the stationary points were characterized by analytical frequency calculations, i.e., energy minima (reactants, intermediates, and products) must exhibit only positive harmonic frequencies, whereas each energy maximum, transition states (TSs), exhibits one and only one negative frequency. From these last calculations, zero-point energy (ZPE), thermal, and entropy corrections were obtained, which were added to the electronic energy to express the calculated values as Gibbs free energies at 298 K and 1 atm.

Our calculations were also performed to include the solvent effect through the PCM model using the SMD parameters according to Truhlar's model[17] with acetonitrile (MeCN) as the solvent. To improve the numerical results, single-point calculations were carried out on the gas-phase optimized geometries using a mixed basis set of triple-ζ quality with one polarization function, 6-311G(d,p), for all the atoms except Br and I, which were treated with the LANL08d relativistic pseudopotential.[18] These energies were added to the gas-phase calculations reported as the final energy values. As a result, the composite level of theory is the following: (SMD: MeCN) ω-B97XD/(6-311G(d,p),LANL08d)//ω-B97XD/6-31G(d).

3. Results and discussion

3.1. Chlorination Mechanism

The calculated mechanism for the chlorination reaction started with coordinating one oxygen of PIFA to aluminum trichloride. This generates a highly exergonic adduct PIFA-$AlCl_3$. In Figure 1, this adduct is set as cero for more clarity. Herein, one chlorine atom is transferred from the aluminum to the hypervalent iodine(III) center through a six-member-ring transition state (**$TS_{1\text{-}Cl}$**, $\Delta G^{\ddagger}$= 9.7 kcal/mol) (selected lengths in such states are 2.76, 1.22, 1.27, 1.78, 2.60, and 2.86 Å for I-O, O-C, C-O, O-Al, Al-Cl, and Cl-I, respectively). Then, the tetracoordinate TFAO-$AlCl_2$ salt is released, giving rise to the intermediate **I-1-Cl** (ΔG= -25.8 kcal/mol), which contains the key Cl-I^{III} bond in a formal $TFAO^-$ / ^-Cl ligand exchange. The Cl-I bond length is 2.46 Å, with the halogen sharing the iodine hypervalent bond in the equatorial position. Next, the second equivalent of aluminum trichloride coordinates to the last $TFAO^-$ ligand, forming the chlorinating active species **I-2-Cl** (ΔG= -18.3 kcal/mol). This favorable energetic step is in equilibrium with its ionic pair (**I-3-Cl**, ΔG= -0.5 kcal/mol). It is worth mentioning that this slight difference in energy between both states means the importance of the spontaneous interconversion of both species, which is observed only in the presence of two chemical equivalents of the Lewis acid.

Afterward, the 2-naphthol addition gets the introduction of the chlorine atom in the phenolic ring, producing the non-aromatic intermediate (**I-4-Cl**, ΔG= -23.1 kcal/mol). Next, the aromatization assisted by TFAO-$AlCl_2$ via (**$TS_{2\text{-}Cl}$**, $\Delta G^{\ddagger}$= 11.1 kcal/mol) and the hydrogen transfer from the non-aromatic intermediate to the TFAO-$AlCl_2$ is observed. In the **$TS_{2\text{-}Cl}$**, the energetic barrier must be overcome to give rise to the 1-chloro-2-napthol adduct with TFA-OH-$AlCl_2$ (**I-5-Cl**, ΔG= -2.6 kcal/mol) that spontaneously yields the final **1-chloro-2-naphthol** (P-Cl) with concomitant releasing of TFAO-$AlCl_2$ in a highly exothermic process (ΔG= -44.2 kcal/mol) (Figure 1).

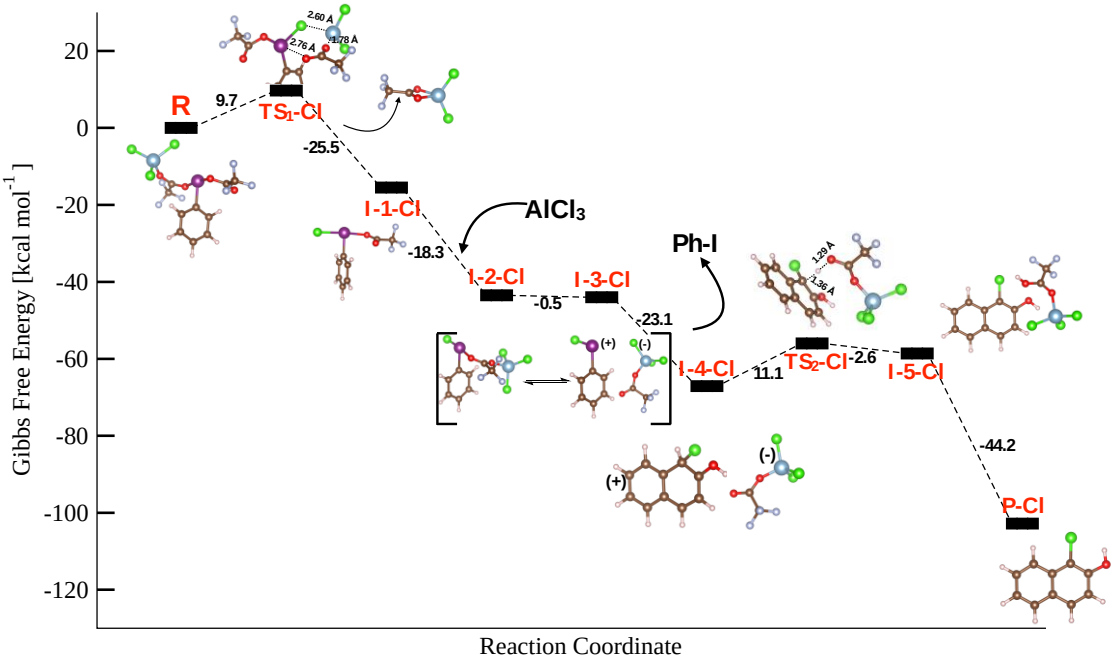

Figure 1. Energy profile for the chlorination of 2-naphthol in the presence of PIFA and $AlCl_3$. The Gibbs free energy values are in kcal/mol.

Other relevant routes for this chlorination process, which involves different stoichiometries or the formation of $PhICl_2$ as a chlorinating species, were also investigated and ruled out. Thus, for the chlorination of 2-naphthol under the PIFA-$AlCl_3$ (1:1) system (see SI for details of the explored chlorination and bromination mechanisms), we found, in general, that once the intermediate **I-1-Cl** is formed, the following coordination of 2-naphthol with the $TFAO^-$ ligand via the **TS2** is energetically less favorable ($\Delta G^{\ddagger}$= 16.2 kcal/mol). Additionally, for this explored mechanism, we identified that the formation of the **TS4** is the largest energetic barrier ($\Delta G^{\ddagger}$= 20.2 kcal/mol), becoming a less probable route. This result also confirms the relevance of using two equivalents of aluminum trichloride.

Regarding the aromatic chlorination using iodine(III) reagents, this reaction is broadly dominated using $PhICl_2$.[1g.] Thus, we explored two alternatives for chlorinating 2-naphthol that could yield 1-Cl-2Np-OH via the $PhICl_2$ formation to identify or rule out this plausible reaction pathway. The first explored mechanism using PIFA-$AlCl_3$ and the second mechanism involved the reaction of PIDA-$AlCl_3$ (shown in SI, Figures S3 and S4, respectively). For both cases, the route was driven to the formation of the $PhICl_2$ as the chlorinating reagent by considering 2 equivalents of $AlCl_3$ [(PIFA or PIDA)-$AlCl_3$ (1:2)].

Overall, we characterized four **TSs** along the reaction coordinate for both pathways. Although the PIFA-assisted mechanism follows a similar route to that described in Figure 1 until the formation of the chlorinating active species, for this case, the formation of the **TS_2** requires 18.1 kcal/mol, which makes a process energetically higher concerning the equilibrium found between **I-2-Cl** and its ionic pair **I-3-Cl** proposed as chlorinating active species in Figure 1, which requires less than 1 kcal/mol. It is worth mentioning that, once $PhICl_2$ is formed, the energetic barrier to **TS3** is 21.5 kcal/mol. These findings suggested that these energetic differences make it less viable the traceroute $PhICl_2$ for the chlorination of 2-naphthol.

On the other hand, in the presence of PIDA (see SI, Figure S4), when the reaction occurs through the chlorination species $PhICl_2$, we found that the **TS_1, TS_2**, and **TS_4** required 17.7, 13.8, and 16.5 kcal/mol, respectively. Considering, that the largest **TS** barrier in the proposed mechanism shown in Figure 1 for **TS2-Cl** = 11.1 kcal/mol, is less probable. Additionally, we observed that the chlorination of naphthol (the formation of **I-6**) could be the determining step since we found a coupling between the ring of the chlorinating species and the naphthol during **TS4**, i.e., it could unfavored the PIDA-assisted chlorination traceroute via $PhICl_2$.

Thus, using PIFA and two equivalents of $AlCl_3$ resulted in the best-yielding reagent and stoichiometry, which agrees with our experiments.

As a consequence of the previous analysis, the chlorination process is energetically more favorable in the presence of PIFA and $AlCl_3$ in a (1:2) ratio, through the formation of the [PhICl(TFAO-$AlCl_3$] in equilibrium with $[PhICl]^+$ -[TFAO-$AlCl_3$] as chlorinating species.

To conclude this section, the general calculated mechanism is described in Scheme 2.

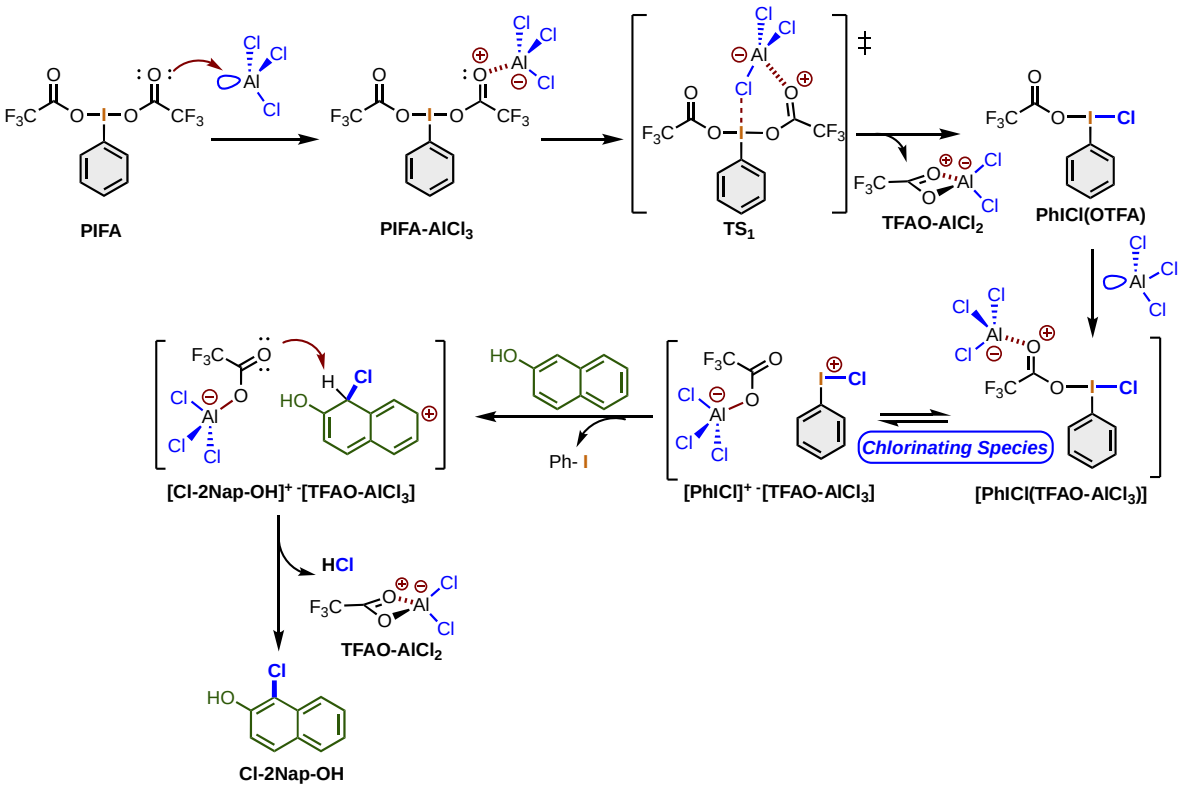

Scheme 2. Calculated reaction mechanism for the chlorination of 2-naphthol using the PIFA/$AlCl_3$ (1:2) system.

PIFA coordinates the first equivalent of aluminum trichloride to get the corresponding adduct **PIFA-$AlCl_3$**. Next, a chlorine atom is transferred to the iodine(III) center to yield **PhICl(OTFA)** via **TS_1** with the release of the complex **TFAO-$AlCl_2$**.Then, the second equivalent of aluminum trichloride coordinates the last trifluoroacetate ligand, giving rise to the chlorinating species **[PhICl(TFAO-$AlCl_3$)]** in equilibrium with **$[PhICl]^+$ $^-$[TFAO-$AlCl_3$]**. At this point, the 2-naphthol reacted, leading to the formation of **[Cl-2Nap-OH]+ -[TFAO-$AlCl_3$],** which after the release of the second **TFAO-$AlCl_2$** complex, yielded the final product **1-chloro-2-napthol**

3.2. Bromination mechanism

The bromination reaction proceeds by a stepwise mechanism. Regarding our calculations, the reaction started with the coordination of the aluminum tribromide to one acetate ligand in PIDA to get the [PIDA-$AlBr_3$] adduct in a highly exergonic process. Similarly to the

previous section, this point was set to zero as a reference. At this stage, the [PIDA-$AlBr_3$] adduct carried out an ionization, giving rise to the corresponding ionic pair (**I-1-Br**, ΔG= -31.3 kcal/mol) in a very exergonic and favorable process. Next, an intramolecular SN_2 reaction in the formed aluminum anion, it transfers a bromine atom to the electrophilic iodine(III) center through **TS_1-Br** that has a feasible energy barrier of 8.3 kcal/mol. The I-Br and Br-Al lengths are 3.15 and 2.78 Å, respectively, and the I-Br-Al angle is 93.1º, quite close to the common T-shape of these hypervalent iodine(III) atoms. This step releases the tetracoordinate AcO-$AlBr_2$ salt and gives rise to the intermediate (**I-2-Br**, ΔG= -9 kcal/mol), which contains the key Br-I^{III} bond with a longitude of 2.65 Å. Herein, we can identify an energetically favorable AcO- / Br- ligand exchange that releases 35.2 kcal/mol. At this point, the second equivalent of aluminum tribromide is coordinated with the last acetate ligand to produce the brominating active species **I-3-Br** [Br-I(Ph)-OAc-$AlBr_3$]. Then, the 2-naphthol carries an *O*-attack over the iodine(III) center to release the activated [Br_3Al-OAc]- ligand through the transition state **$TS_{2\text{-}Br}$** ($\Delta G^{\ddagger}$ = 11.7 kcal/mol), which leads to the protonated intermediate **I-4-Br**. The next step is a deprotonation assisted by the released [Br_3Al-OAc] species. This allows the formation of the AcO-$AlBr_2$ salt via **$TS_{3\text{-}Br}$** and the *trans*-intermediate (**I-5-Br**), which contains the Br-I(Ph)-O-Nph bond (2.14 Å). The last step is the bromination of **I-5-Br** by isomerization to the *cis*-transition state (**$TS_{4\text{-}Br}$**, $\Delta G^{\ddagger}$ = 16.1 kcal/mol), which yields the brominated non-aromatic intermediate **I-6-Br** in a highly exothermic step which with a DG= -52.3 kcal/mol. Finally, **I-6-Br** undergoes a spontaneous aromatization that converts it into the experimentally observed **1-bromo-2-naphthol** (P-Br), which is 2.6 kcal/mol more stable than **I-6-Br** (Figure 2).

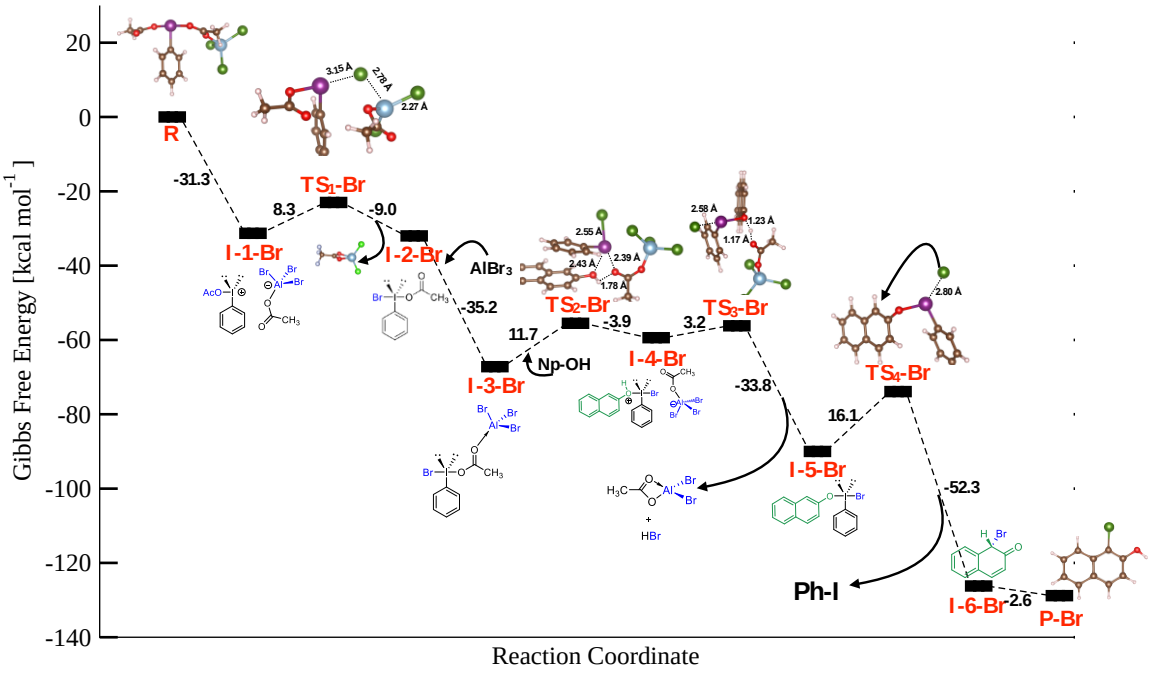

Figure 2. Calculated mechanism for the bromination of 2-naphthol in the presence of PIDA and $AlBr_3$. The Gibbs free energy values are in kcal/mol.

We also explored the mechanisms for the bromination of 2-naphthol mediated by PIFA in a (1:2) ratio (shown in Figure S5). From this proposal, we observe that the energetic barrier to reach **TS1** (10.6 kcal/mol) and **TS2** (16.7 kcal/mol) are larger than those calculated from the mechanism shown in Figure 2 [$\mathbf{TS_{1\text{-}Br}}$ (8.3 kcal/mol) and $\mathbf{TS_{4\text{-}Br}}$ (16.1 kcal/mol)], respectively.

Other possible mechanisms could be through the formation of $PhIBr_2$; for such cases, we obtained the pathways concerning the PIDA and PIFA by using 2 equivalents of $AlBr_3$, respectively (see Figures S6-7). The calculations indicated these pathways proceed along four transition states each. Moreover, we found that the coordination of the $AlBr_3$ - **I-2** to form $\mathbf{TS_2}$ is the largest energetic barrier (determining step, $\mathbf{TS_2}$, $\Delta G^{\ddagger}$ = 53.3 kcal/mol) in the presence of PIDA. Meanwhile, the formation of the $\mathbf{TS_3}$, $\Delta G^{\ddagger}$ = 21.3 kcal/mol is the limiting step of the mechanism in the presence of PIFA.

Then, in the presence of the PIFA–$AlBr_3$ system, the bromination of 2-naphthol is the most energetically favorable pathway. Although all these reactions occur through four transition states, significant energetic differences exist concerning the PIDA-$AlBr_3$ system. For example, the activation barrier of $\mathbf{TS_2}$ is 41.6 kcal/mol higher in energy than that of the

mechanism of Figure 2. A similar energetic profile is shown for the bromination of 2-naphthol in the presence of PIFA (2 eq $AlBr_3$) compared with those in Figure 2. The energy difference between **I-1** to **TS_1** (2.3 kcal/mol for the reaction in the presence of PIFA) could be the reason why the experimentally obtained yields by considering the different hypervalent iodine reagents for this reaction are more favorable in the presence of PIDA-$2AlBr_3$ than PIFA-$2AlBr_3$.

To find the correlation degree between experimental and theoretical calculations, it was carried out the chlorination and bromination of 2-naphthol using the PIFA-AlCl3 system or PIDA-AlBr3 system respectively. We found an excellent correlation between each mechanism yielding and energy barriers shown in Table 1.

Table 1. Experimental yields by using different hypervalent iodine(III) reagents

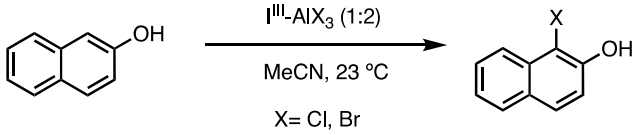

Reaction	**I^{III}**		**AlX_3**
	PIFA	**PIDA**	
Chlorination	**63%**	48%	**$AlCl_3$**
Bromination	84%	**93%**	**$AlBr_3$**

To conclude this section, the general proposed mechanism is detailed in Scheme 3.

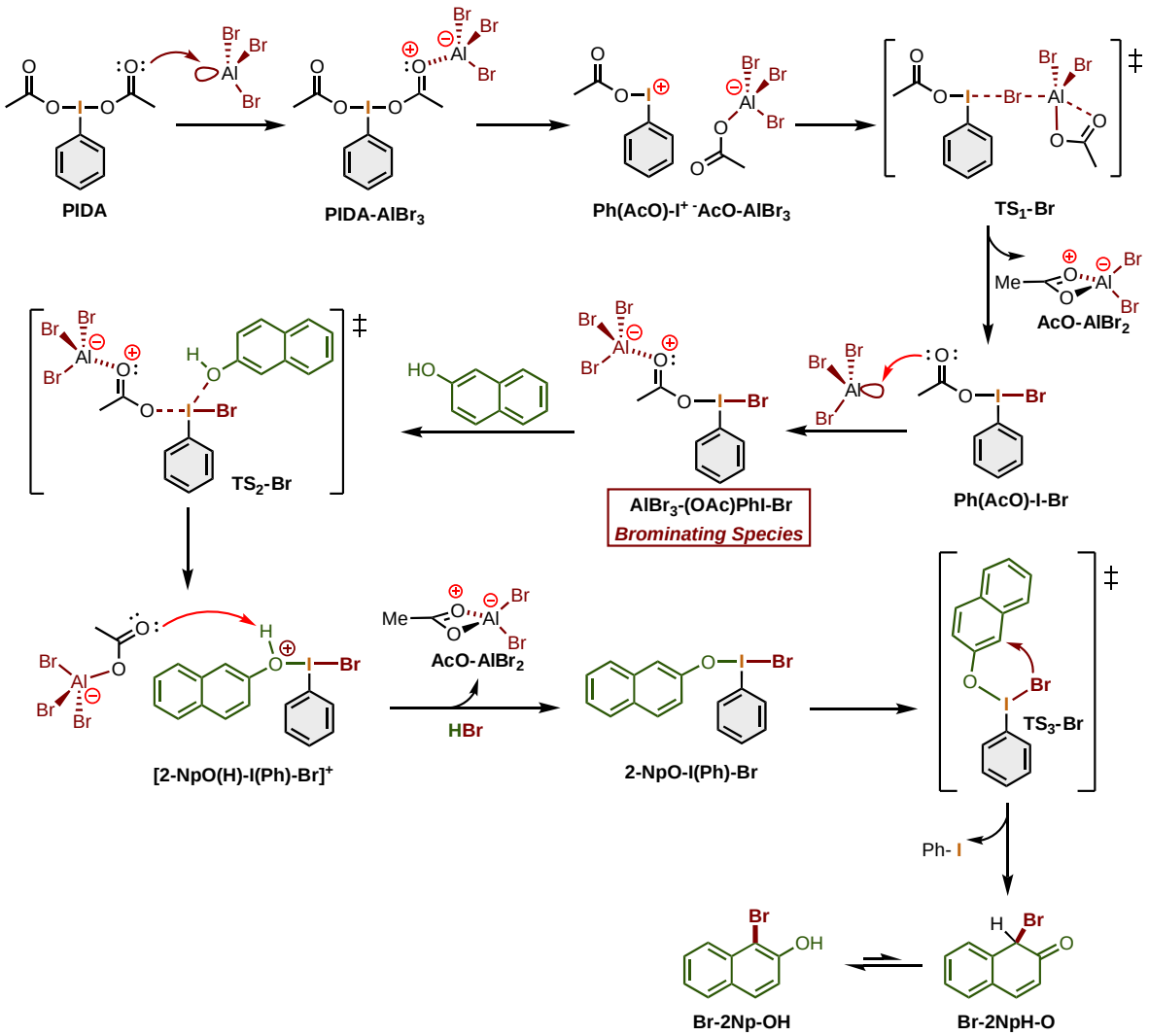

Scheme 3. Calculated reaction mechanism for the bromination of 2-naphthol using the PIDA/$AlBr_3$ (1:2) system.

PIDA coordinates the first equivalent of aluminum tribromide to get the adduct **PIDA-$AlBr_3$**, which spontaneously dissociates, giving the ionic pair **Ph(AcO)$^+$ -AcO-$AlBr_3$**. Next, via **TS_1-Br**, the complex **AcO-$AlBr_2$** is released with the subsequent formation of intermediate **Ph(AcO)-I-Br**. Then, the second equivalent of aluminum tribromide coordinates to the last acetate ligand, forming the adduct $AlBr_3$-(OAc)PhI-Br, i.e., the brominating species. At this point, the 2-naphthol reacted and led to the formation of **[2-[NpO(H)-I(Ph)-Br]$^+$** via **TS_2-Br**. Afterward, the second equivalent of the **AcO-$AlBr_2$** complex and HBr is released with concomitant formation of **2-NpO-I(Ph)-Br**. Finally, through the transition state **TS_3-Br**, the

intermediate **Br-2NpH-O** is formed, which is in equilibrium with the experimentally observed **Br-2Np-OH**.

Conclusions

We elucidated the most energetically viable pathway for the chlorination and bromination of 2-naphthol using the novel systems PIFA-$AlCl_3$ and PIDA-$AlBr_3$ in a (2:1) ration for both cases. We found that the most energetically favorable reaction leads through the chlorinating species involving an equilibrium between the Cl-I(Ph)-OTFA-$AlCl_3$ and [Cl-I(Ph)+] [-OTFA-$AlCl_3$] species more than the $PhICl_2$ formation. The bromination mechanism is more efficient with PIDA and $AlBr_3$ through the formation of the intermediate Br-I(Ph)-OAc-$AlBr_3$ as the brominating active species. Similarly, the $PhIBr_2$ is less energetically favorable than our proposal. One key step is the coordination of a second equivalent of AlX_3 to the last TFAO- or AcO- in the PIFA or PIDA to promote the formation of the halogenating active species (**I-2** and **I-3** for chlorination and bromination, respectively). Although the bromination reactions in the presence of PIDA and PIFA give excellent experimental yielding, slight energy differences in the pathways explain why the PIFA-$AlCl_3$ for chlorination and PIDA-$AlBr_3$ for bromination are the better choices for these reactions.

Supporting Information

Optimized Cartesian coordinates of all the structures involved in the reaction mechanisms and the variation of the reaction pathways explored.

Notes

The authors declare no competing financial interests.

Acknowledgements

K.A.J.-O. thanks to CONAHCyT for financial support (PhD fellowship). We acknowledge the facilities of the DCNyE, the Chemistry Department, and the Supercomputing Center facilities of the National Laboratory UG-CONACyT (LACAPFEM) of the University of

Guanajuato. We also thank Fernando Murillo for the kind discussion. This work is dedicated to the memory of our friend Kevin Juarez who unfortunately passed away.

References

(1) a) Yoshimura, A.; Zhdankin, V. V. *Chem. Rev.* **2016**, *5*, 3328–3435. b) Zhdankin, V. V. *ARKIVOC* **2009**, *1*, 1–62. c) Zhdankin, V. V. *Hypervalent Iodine Chemistry: Preparation, Structure and Synthetic Applications of Polyvalent Iodine Compounds*, WILEY–VHC: New York, 2014. d) Chávez-Riera, R.; Navarro-Santos, P.; Chacón-García, L.; Ortíz-Alvarado, R.; Solorio-Alvarado, C. R. *ChemistrySelect*, **2023**, *8*, e202303425. e) Segura-Quezada, L. A.; Torres-Carbajal, K. R.; Juárez-Ornelas, K. A.; Navarro-Santos, P.; Granados-López, A. J.; Ortíz-Alvarado, R.; de León-Solís, C.; Solorio-Alvarado, C. R. *Curr. Org. Chem.* **2022**, *26*, 1954-1968. f) Kikushima, K.; Elboray, E. E.; Jiménez-Halla, J. O. C.; Solorio-Alvarado, C. R.; Dohi, T. *Org. Biomol. Chem.* **2022**, *20*, 3231-3248. g) Segura-Quezada, L. A.; Torres-Carbajal, K. R.; Juárez-Ornelas, K. A.; Alonso-Castro, A. J.; Ortíz-Alvarado, R.; Dohi, T.; Solorio-Alvarado, C. R. *Org. Biomol. Chem.* **2022**, *20*, 5009-5034. h) Segura-Quezada, L. A.; Torres-Carbajal, K. R.; Satkar, Y.; Juárez Ornelas, K. A.; Mali, N.; Patil, D. B.; Gámez-Montaño, R.; Zapata-Morales, J. R.; Lagunas-Rivera, S.; Ortíz-Alvarado, R.; Solorio-Alvarado, C. R. *Mini-Reviews in Organic Chemistry*, **2021,** *18*, 1-14.

(2) Wang, B.; Graskemper, J. W.; Qin, L.; DiMagno, S. G. *Angew. Chem. Int. Ed.* **2010**, *49*, 4079–4083.

(3) a) Segura-Quezada, L. A.; Torres-Carbajal, K. R.; Mali, N.; Patil, D. B.; Luna-Chagolla, M.; Ortíz-Alvarado, R.; Tapia-Juárez, M.; Fraire-Soto, I.; Araujo-Huitrado, J. G.; Granados-López, A. J.; Gutiérrez-Herández, R.; Reyes-Estrada, C. A.; López-Hernández, Y.; López, J. A.; Chacón-García, L.; Solorio-Alvarado, C. R. *ACS Omega*, **2022**, *7*, 6944-6955. b) Nahide, P. D.; Jiménez-Halla, J. O. C.; Wrobel, K.; Solorio-Alvarado, C. R.; Ortíz-Alvarado, R.; Yahuaca-Juárez, B. *Org. Biomol. Chem.* **2018**, *16*, 7330-7335.

(4) a) Kita, Y.; Dohi, T.; Morimoto, K. *Yuki Gosei Kagaku Kyokaishi* **2011**, *69*, 1241−1250. b) Yuvraj, S.; Wröbel, K.; Trujillo-González, Daniel E.; Ortíz-Alvarado, R.; Jiménez-Halla, J. O. C.; Solorio-Alvarado, C. R. *Front. Chem.*, **2020**, *8*:563470.

(5) a) Dohi, T.; Maruyama, A.; Yoshimura, M.; Morimoto, K.; Tohma, H.; Kita, Y. *Angew Chem Int Ed Engl*. **2005**, *44*, 6193–6196. b) Yahuaca-Juárez, B.; González, G.; Ramírez-Morales, M. A.; Alba-Betancourt, C.; Deveze-Álvarez, M. A.; Mendoza-Macías, C. L.; Ortíz-Avarado, R.; Juárez-Ornelas, K. A.; Solorio-Alvarado, C. R.; Maruoka, K. *Synth. Commun.*, **2020**, *50*, 539-548.

(6) Dohi, T.; Maruyama, A.; Minamitsuji, Y.; Takenaga, N.; Kita, Y. *Chem. Commun.*, **2007**, 1224–1226.

(7) Kumar, R. K.; Manna, S.; Mahesh, D.; Sar, D.; Punniyamurthy, T. *Asian J. Org. Chem*. **2013**, *2*, 843–847.

(8) Dohi, T.; Morimoto, K.; Takenaga, N.; Goto, A.; Maruyama, A.; Kiyono, Y.; Tohma, H.; Kita, Y. *J. Org. Chem*. **2007**, *72*, 109–116.

(9) a) Karam, O.; Jacquesy, J.C.; Jouannetaud M.P. *Tetrahedron Lett.*, **1994**, *35*, 2541-2544. b) Zhao, Z.; To, A.J.; Murphy, G.K. *Chem. Commun. (Camb.)*, **2019**, *55*, 14821-14824.

(10) a) Mali, N.; Ibarra-Gutiérreez, J. G.; Lugo-Fuentes, L. I.; Ortíz-Alvarado, C. R.; Chacón-García, L.; Navarro-Santos, P.; Jiménez-Halla, J. O. C.; Solorio-Alvarado, C. R. *Eur. J. Org. Chem.* **2022**, e202201067. b) Satkar, Y.; Yera-Ledesma, L. F.; Mali, N.; Patil, D.; Navarro-Santos, P.; Segura-Quezada, L. A.; Ramírez-Morales, P. I.; Solorio-Alvarado, C. R. *J. Org. Chem.* **2019**, *84*, 4149-4164.

(11) a) Patil, D. P.; Gámez-Montaño, R.; Ordoñez, M.; Solis-Santos, M.; Jiménez-Halla, J. O. C.; Solorio-Alvarado, C. R. *Eur. J. Org. Chem.* **2022**, e202201295. b) Juárez-Ornelas, K. A.; Jiménez-Halla, J. O. C.; Kato, T.; Solorio-Alvarado, C. R.; Maruoka, K. *Org. Lett.* **2019**, *21*, 1315-1319.

(12) a) Nahide, P.D.; Ramadoss, V.; Juárez-Ornelas, K.A.; Satkar, Y.; Ortiz-Alvarado, R.; Cervera-Villanueva, J. M. J.; Alonso-Castro, A.J.; Zapata-Morales, J. R.; Ramírez-Morales, M.A.; Ruiz-Padilla, A.J.; Deveze-Álvarez, M.A.; Solorio-Alvarado, C. R. *Eur. J. Org. Chem.,* **2018**, 485-493. b) Cheng, D.; Chen, Z.; Zheng, Q. *J. Chem. Res.,* **2002**, 624-625. c) Satkar, Y.; Ramadoss, V.; Nahide, P.D.; García-Medina, E.; Juárez-Ornelas, K.A.; Alonso-Castro, A. J.; Chávez-Rivera, R.; Jiménez-Halla, J. O. C.; Solorio-

Alvarado, C.R. *RSC Advances*, **2018**, *8*, 17806-17812. d) Segura-Quezada, L. A.; Satkar, Y.; Patil, D.; Mali, N.; Wröbel, K.; González, G.; Zárraga, R.; Ortíz-Alvarado, R.; Solorio-Alvarado, C. R. *Tetrahedron Lett.* **2019**, *60*, 1551-1555.

(13) Evans, P.A.; Brandt, T.A. *Tetrahedron Lett.*, **1996**, *37*, 6443-6446.

(14) Granados, A.; Shafir, A.; Arrieta, A.; Cossío, F. P.; Vallrribera, A. *J. Org. Chem.*, **2020**, *85*, 2142–2150.

(15) Frisch, M. J.; Trucks, G. W.; Schlegel, H. B.; Scuseria, G. E.; Robb, M. A.; Cheeseman, J. R.; Scalmani, G.; Barone, V.; Petersson, G. A.; Nakatsuji, H.; Li, X.; Caricato, M.; Marenich, A.; Bloino, J.; Janesko, B. G.; Gomperts, R.; Mennucci, B.; Hratchian, H. P.; Ortiz, J. V.; Izmaylov, A. F.; Sonnenberg, J. L.; Williams-Young, D.; Ding, F.; Lipparini, F.; Egidi, F.; Goings, J.; Peng, B.; Petrone, A.; Henderson, T.; Ranasinghe, D.; Zakrzewski, V. G.; Gao, J.; Rega, N.; Zheng, G.; Liang, W.; Hada, M.; Ehara, M.; Toyota, K.; Fukuda, R.; Hasegawa, J.; Ishida, M.; Nakajima, T.; Honda, Y.; Kitao, O.; Nakai, H.; Vreven, T.; Throssell, K.; Montgomery, J. A.; Peralta, Jr.; J. E.; Ogliaro, F.; Bearpark, M.; Heyd, J. J.; Brothers, E.; Kudin, K. N.; Staroverov, V. N.; Keith, T.; Kobayashi, R.; Normand, J.; Raghavachari, K.; Rendell, A.; Burant, J. C.; Iyengar, S. S.; Tomasi, J.; Cossi, M.; Millam, J. M.; Klene, M.; Adamo, C.; Cammi, R.; Ochterski, J. W.; Martin,R. L.; Morokuma, K.; Farkas, O.; Foresman, J. B.; Fox, D. J. Gaussian, Inc., Wallingford CT, 2009. Gaussian 16, Revision C. 01.

(16) Chai, J.-D.; Head-Gordon, M. *Phys. Chem. Chem. Phys.* **2008**, *10*, 6615-6620.

(17) (a) Marenich, A. V.; Cramer, C. J.; Truhlar, D. G. *J. Phys. Chem. B* **2009**, *113*, 6378. (b) Barone V.; Cossi, M. *J. Phys. Chem. A* **1998**, *102*, 1995. (c) Cossi, M.; Barone, V.; Mennucci, B.; Tomasi, J. *Chem. Phys. Lett.* **1998**, *286*, 253. (d) Barone, V.; Cossi, M. ; Tomasi, J. *J. Comp. Chem.* **1998**, *19*, 404. (e) Tomasi, J.; Mennucci, B.; Cammi, R.*Chem. Rev.* **2005**, *105*, 2999.

(18) (a) Wadt, W. R.; Hay, P. J. *J. Chem. Phys.* **1985**, *82*, 284. (b) Hay P. J.; Wadt, W. R. *J. Chem. Phys.* **1985**, *82*, 299. (c) Roy, L. E.; Hay, P. J.; Martin, R. L. *J. Chem. Theory Comput.* **2008**, *4*, 1029.